

An Omnidirectional Antenna with Multi-taper Conformal Structure

Zhaoneng Jiang^{1,2}, Yongxin Sha¹, Xiaofeng Xuan¹, and Liying Nie¹

¹School of Electronic Science and Applied Physics
Hefei University of Technology, Hefei, 230009, China

²National Mobile Communications Research Laboratory
Southeast University, Jiangsu, 210096, China
jiangzhaoneng@hfut.edu.cn

Abstract – In this paper, a wideband quadrangular pyramid conformal printed dipole antenna is designed, manufactured, and tested. The proposed antenna comprises four dipoles pointing in different directions and four pairs of parasitic patches. Each dipole and pair of parasitic patches are placed on one side of the pyramid. The simulated impedance bandwidth exceeds 26% ($S_{11} \leq -10$ dB), with the conformal taper varied from 0° to 20° . Omnidirectional radiation characteristics can be realized within the working bandwidth. The prototype of the proposed antenna with 10° taper is fabricated and measured. Moreover, the results show that the operating frequency band is 2.28–3.58 GHz in the S-band. The size of the fabricated antenna is 35×35 mm². The conclusion is that the simulation and test results of the 10° taper antennas are highly consistent.

Index Terms – conformal, multi-taper, omnidirectional.

I. INTRODUCTION

To achieve communication, detection, navigation, and other functions, various antenna types are required for a single piece of equipment. The advantage of reducing the influence on the aerodynamic performance of mobile carriers was shown by the conformal antenna due to it fitting closely to the surface of the equipment. They have therefore been widely used in military and civilian applications such as unmanned aerial vehicles [1], missile heads, borehole radar [2], global satellite navigation systems (GSNS) [3], wearable devices [4], vehicle-borne devices [5, 6], and other wireless communication terminal devices that need a conformal configuration [7]. A conformal antenna with strong adhesion and integrated design has since become one of the research hotspots in the field of antennae.

Omnidirectional radiation antennae are widely used in short-range detection, scanning, and so on because of their wide beamwidth and radiation coverage. Com-

pared with directional antennae, which can only receive radiation signals in a specified direction, omnidirectional antennae do not have strict requirements on the azimuth of the transmitted signal. This dramatically improves the efficiency of short-distance signal transmission. The combination of traditional omnidirectional antenna and conformal antenna design significantly expands the application of such antennae in the area of detection. A bipolar omnidirectional antenna conformal to the capsule surface for endoscopy systems is presented in [8]. However, the proposed antenna has a high specificity for application due to the capsule shape of the conformal carrier and the low gains effect. A characteristic mode analysis (CMA)-based omnidirectional microstrip antenna conformal to different radians is presented in [9]. The designed broadband circularly polarized (BCP) antenna unit can achieve 35.6% impedance bandwidth and 22% circularly polarized bandwidth under different bending radii along the x- and y-axes. However, the omnidirectional radiation characteristics of the antenna mainly depend on the radian of the carrier and the number of antenna units. In order to obtain low gain variation in the horizontal plane, a conformal array antenna requires more elements, which complicates the antenna feeding network. To simplify the design complexity of the conformal omnidirectional antenna and widen the impedance bandwidth of the antenna, a multiband antenna based on inkjet-printing is proposed in [10]. The operating bandwidth of the antenna can cover Global Positioning Systems (GPS), Wireless Local Area Networks (WLAN), Bluetooth, and other bands. The relative bandwidth can reach 54.4%, 14%, 23.5%, and 17.2%, respectively. At the same time, due to the conformality of the inkjet-printed antenna, the experimental results show that the impedance bandwidth of the antenna is basically unchanged, and the omnidirectional radiation gain is above -1.2 dBi with cylinder radii of 78 mm and 59 mm. To obtain higher radiation gain, an omnidirectional conformal antenna based on dipole form is

proposed in [11]. The antenna can achieve a maximum circular polarized radiation gain of 5.2 dBi within the relative impedance bandwidth of 55.8%. Besides, the radiation performance of the antenna is studied, which is conformal to the cylindrical section with a horizontal downward oblique angle of 0° - 30° , respectively.

In order to further simplify the antenna structure based on the design of the document [11] and reduce the antenna design size, the antenna can be adapted to different conformal tapers. A conformal dipole antenna with omnidirectional radiation characteristics is presented in this paper. The experimental simulation results show that the antenna can achieve omnidirectional radiation characteristics in the full bandwidth when the pyramid taper varies from 0° to 20° . The radiation gain is higher than 1dB in the working bandwidth.

The main innovation of this paper is to design an omnidirectional radiation antenna based on bent arm dipoles. By introducing a parasitic patch, the bandwidth of the omnidirectional antenna is extended, and the conformal of the antenna on the surface of the pyramid is realized.

This paper is organized as follows. The design and analysis of the antenna are presented in Section II. Experimental results are described in Section III. Finally, the conclusion is given in Section IV.

II. ANTENNA DESIGN AND ANALYSIS

A. Planar omnidirectional antenna design

A multi-view of the proposed omnidirectional antenna is presented in Fig. 1, which comprises four dipoles. A circular low-cost FR4 substrate material ($\epsilon_r = 4.4$) with a height of 0.508 mm is used to print this antenna.

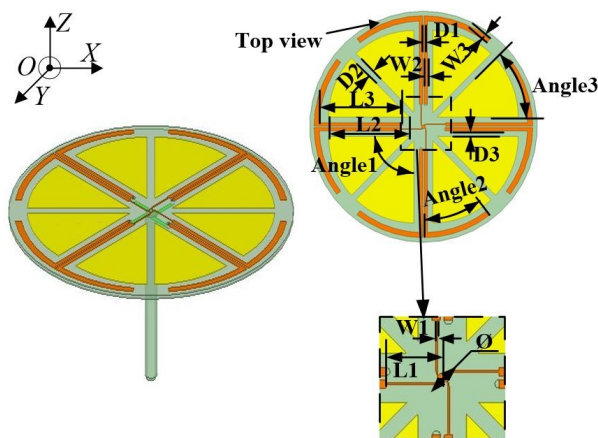


Fig. 1. The structure of the planar antenna.

The dimensions of the microstrip patch antenna in Fig. 1 are optimized by high frequency structure simu-

lator (HFSS) software, and the parameters are shown in Table 1. It can be seen from Fig. 1 that the structure of the antenna is relatively simple, of low cost, and easily applied in practical engineering terms.

Table 1: Dimensions of the proposed antenna element (unit: mm)

Symbol	Value	Symbol	Value
$L1$	7	$D2$	2
$L2$	30	H	0.508
$L3$	33	\emptyset	1.2
$W1$	0.25	$D1$	0.5
$W2$	1	Angle 1	90°
$W3$	1.6	Angle 2	37.5°
$D3$	2.58	Angle 3	30°

The result of the impedance matching is shown in Fig. 2 (b). The inner conductor of the antenna is connected to a microstrip line extending in four directions on the upper surface. The outer is connected to the corresponding microstrip lines on the lower surface and then, through metalized vias, connects the ground line to the upper surface, forming a dipole form with the original microstrip structure. The four microstrip dipoles on the substrate in different directions enable the antenna to obtain specific omnidirectional radiation characteristics.

Figure 3 shows the equivalent circuit of the dipole unit, in which C_f and L_f represent the feeding capacitance and inductance, respectively, and their influence is negligible for the input impedance. When the dipole antenna works in the base model state, the electric dipole can be replaced by a series resonant circuit (resistance R_d , capacitance C_d , and inductance L_d), and the equivalent capacitance of the parasitic patch circuit is C_{pp} , and the inductance is L_{pp} .

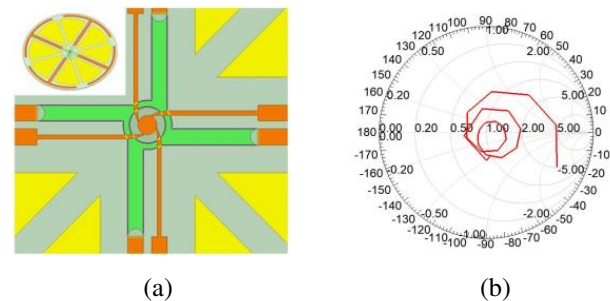


Fig. 2. (a) The impedance matching circuit; (b) the Smith circle of the matching circuit.

To match impedance, an impedance matching circuit is shown in Figs. 2 (a) to connect the 50Ω SubMiniature

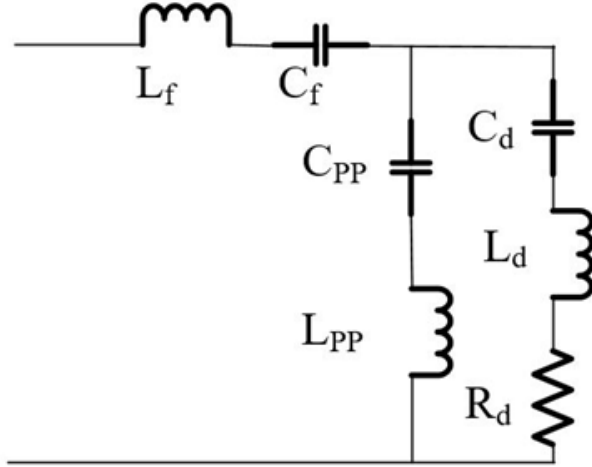


Fig. 3. The equivalent circuit of the dipole unit.

version A (SMA) and radiation patches. The impedance matching circuit of the antenna mainly uses four $\lambda/4$ lines to realize impedance transformation, and its formula is as follows:

$$Z_{in} = Z_0 = \frac{Z_A^2}{Z_A}, \quad (1)$$

where Z_{in} is the input impedance, Z_0 is the characteristic impedance of the transmission line, and Z_A is the impedance of the microstrip antenna.

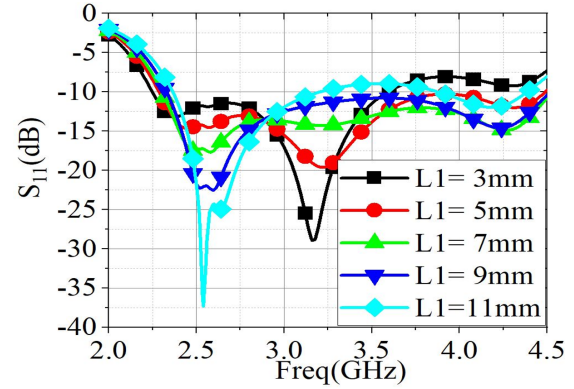
In order to obtain the optimal size for the $\lambda/4$ line, the length and width of the $\lambda/4$ line are simulated and compared, and the results are shown in Fig. 4. Considering the antenna bandwidth and matching depth, the length of the $\lambda/4$ line is 7 mm and the width is 0.25 mm.

Through characteristic mode analysis (CMA) of the planar microstrip structure to accelerate the antenna design cycle. The generalized eigenmode equation is as follows:

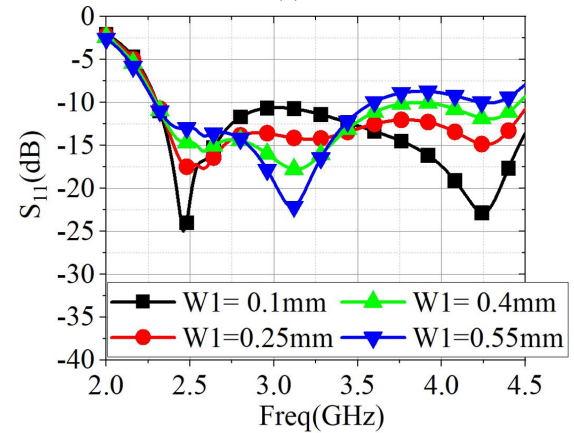
$$XJ_n = \lambda_n R_n J_n, \quad (2)$$

where X is the imaginary part of the impedance matrix, J_n is the eigenvector, R_n is the weighted matrix, and λ_n is the solution of the generalized eigenvalue equation $XJ_n = \lambda_n R_n J_n$. When $\lambda_n = 0$, the energy stored by the electric field and the magnetic field are equal, and the antenna is in a resonance state. When $\lambda_n < 0$, the energy is concentrated in the electric field, and the corresponding mode of the antenna is the capacitive mode. When $\lambda_n > 0$, the energy is focused on the magnetic field, and the corresponding mode of the antenna is the perceptual mode.

The physical meaning of the characteristic angle in the characteristic mode is the phase difference between the characteristic current and the tangential component



(a)



(b)

Fig. 4. (a) Simulated effects of varying the $\lambda/4$ line length; (b) simulated effects of varying the $\lambda/4$ line width.

of the characteristic electric field. The formula is as follows:

$$\beta_n = 180^\circ - \arctan \lambda_n. \quad (3)$$

Since the range of the eigenvalues is $(-\infty, +\infty)$, the range of the characteristic angle is $[90^\circ \leq \beta_n \leq 270^\circ]$. Similarly, the characteristic angle values can be interpreted as follows:

When the eigenvalue is $\lambda_n > 0$, then the range of the eigenvalue angle is $90^\circ < \beta_n < 180^\circ$. The mode is called the inductive mode and stores magnetic energy. When the eigenvalue is $\lambda_n = 0$, then the characteristic angle is $\beta_n = 180^\circ$. The mode is called the resonance mode and the energy radiates outward. When the eigenvalue is $\lambda_n < 0$, the range of the characteristic angle is $180^\circ < \beta_n < 270^\circ$, and the mode is called the capacitive mode, which stores power. When the characteristic angle is 90° or 270° , the mode mainly stores energy and does not radiate outward; that is, it is in an internal resonance state. The phase relationship between modes can be viewed when designing the antenna, so the eigenvalue

parameters are a good guide for the design of circularly polarized or dual-polarized antenna.

The expression for modal significance (MS) is as follows:

$$MS = \left| \frac{1}{1 + j\lambda_n} \right|. \quad (4)$$

The modal significance of the proposed antenna is shown in Fig. 5 (a) and the characteristic angle is shown in Fig. 5 (b). The modal significance of mode 5 exceeds 0.707. Therefore, the omnidirectional property is under the excitation of mode 5. The surface current distribution and the far-field radiation under the excitation of mode 5 are shown in Fig. 6. In order to excite the omnidirectional radiation characteristics and obtain the far-field radiation as shown in Fig. 5 (b), the antenna is excited by an inductive coupling excitation structure (ICE) in the center position.

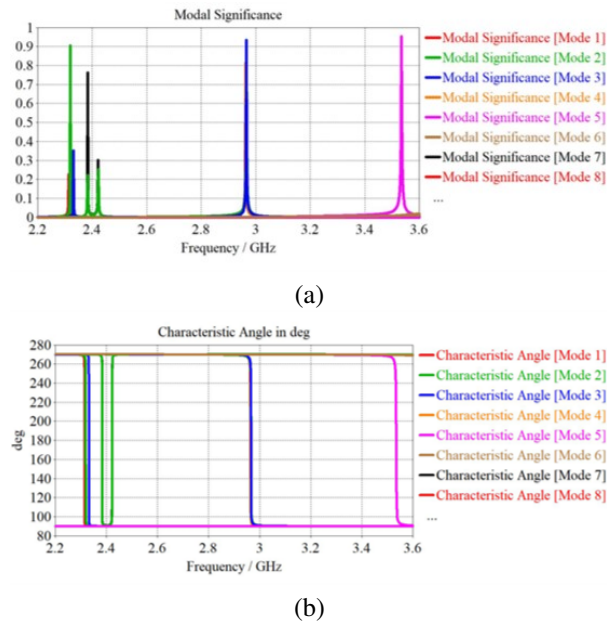


Fig. 5. Characteristic mode analysis: (a) modal significance; (b) characteristic angle.

Broadband technology is one of the key technologies in the design of microstrip antennas. In [12], a defect-based microstrip antenna design for multi-band applications was proposed, which achieves broadband design by introducing parasitic patches. In [13], the effects of separation and gaps in microstrip patches were verified through antenna design. In this design, the antenna bandwidth was successfully expanded by slotting the fan-shaped parasitic patch. Figure 7 is a comparison of the effects on S_{11} parameters of the planar omnidirectional antenna with and without the parasitic patches. It can be seen that the introduction of the parasitic patches makes the antenna introduce new reso-

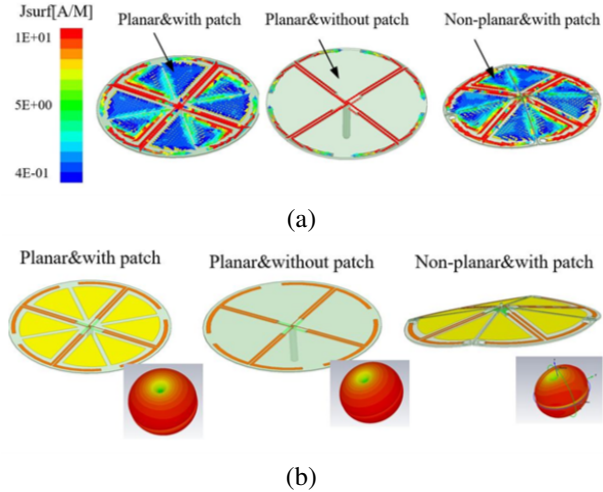


Fig. 6. The results of characteristic mode analysis: (a) the surface current distribution; (b) the far-field radiation.

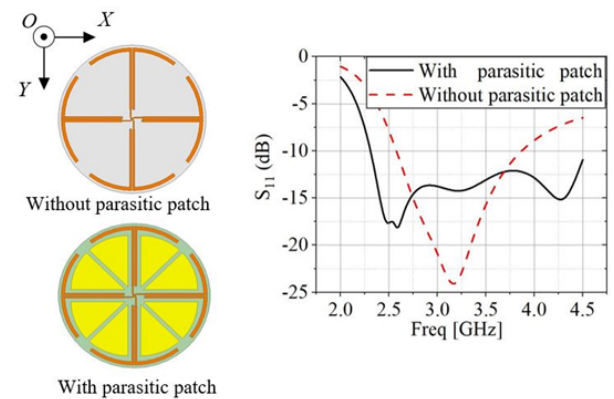


Fig. 7. The effect of parasitic patches on the reflection coefficient of the antenna.

nance points to broaden the reflection coefficient bandwidth of the antenna. The bandwidth of the antenna is increased from 37.6% to 68.6% after the parasitic patch is introduced. In addition, the arm width of the dipole has some influence on the operating frequency band of the antenna. Figure 8 shows the reflection coefficients of a microstrip dipole at different arm widths. It should be noted that, in general, the measured data will deteriorate compared with the simulated data. Therefore, after comparing the reflectivity of dipoles with different arm widths, the 1.6 mm arm widths with higher reflectivity values are selected as the optimal solution for the antenna.

B. Conformal omnidirectional antenna design

The conformal omnidirectional antenna with different pyramid angles will be introduced here. The

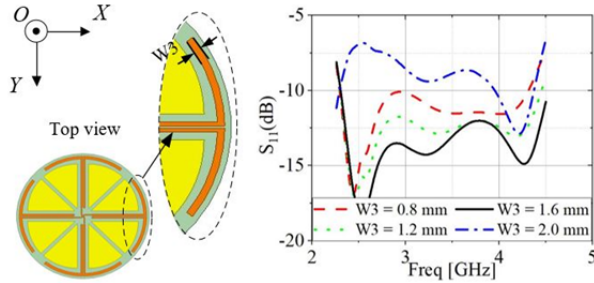


Fig. 8. Simulated effects of varying the arm width of the dipole.

structural diagram of the omnidirectional antenna is shown in Fig. 9. A tube-like structure was used as a carrier for the antenna. This cylinder needs to be hollow in the middle so as to facilitate the soldering of the antenna bottom. It also needs to be perforated in the substrate at a certain height to facilitate the use of a nylon column to fix the conformal antenna. Accordingly, stereolithography appearance (SLA), a 3D printing technology, is used to design the conformal substrate, and epoxy resin with a relative permittivity of 3.5 is selected as the printing material. Polypropylene material with a dielectric constant of 2.2 is used as the fixing bolt in the conformal antenna, which can reduce any interference to the antenna.

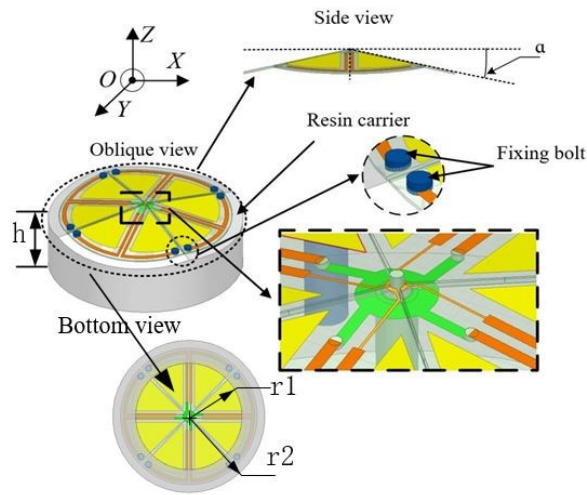
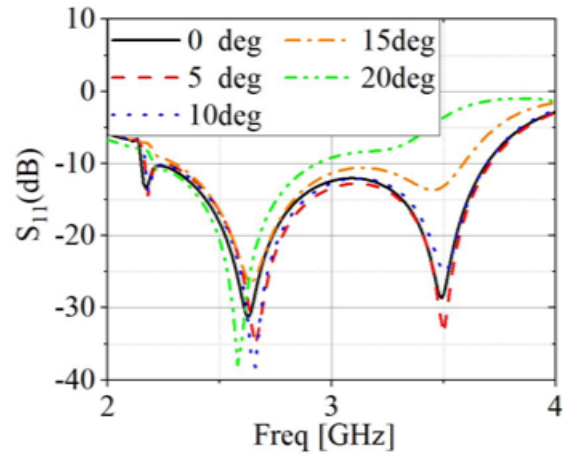
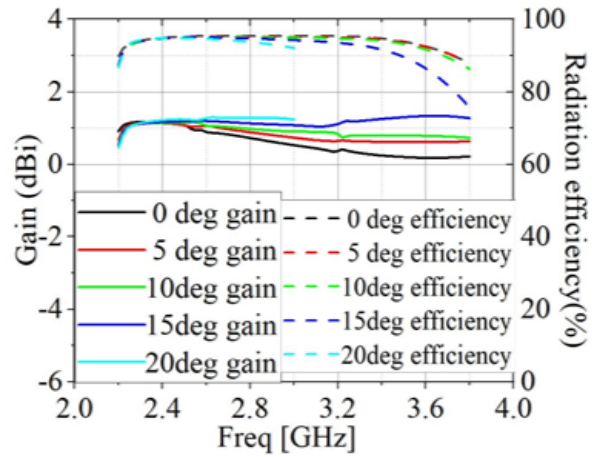


Fig. 9. The structure of the conformal antenna. ($h = 18\text{mm}$, $r1 = 28\text{mm}$, $r2 = 35\text{mm}$).

The simulation results of the reflection coefficient of the omnidirectional antenna under different pyramid angles (α) are shown in Fig. 10 (a). With the pyramid angle increasing from 0° to 15° , the relative bandwidth of the antenna changes from 66% (2.3-4.6 GHz) to 46.7% (2.3-3.7 GHz). When the antenna is conformal to a pyra-



(a)



(b)

Fig. 10. The simulated results of the proposed antenna with different pyramid angles: (a) S_{11} (dB); (b) gain (dBi) and radiation efficiency.

mid with a pyramid angle of 20° , the antenna can achieve a bandwidth of around 26%. The simulation gain and efficiency of the omnidirectional antenna in the working bandwidth are shown in Fig. 10 (b). The maximum simulation gain of the antenna can reach 1dBi, and the gain of the antenna in the whole working bandwidth is more than 0dBi. The simulation efficiency of the antenna with different pyramid angles can reach more than 80% of the effective bandwidth. Figure 11 shows the simulated radiation patterns in E-plane and H-plane at 2 GHz, 2.5 GHz, 3 GHz and 3.5 GHz, respectively. Considering that the working bandwidth of the proposed antenna with the 20° taper is only 26% (2.3-3 GHz), the omnidirectional antenna with a taper of 20° is not simulated and analyzed at 3.5 GHz in Fig. 11. It is clearly seen that the H-plane is omnidirectional from 2 GHz to 3.5 GHz at

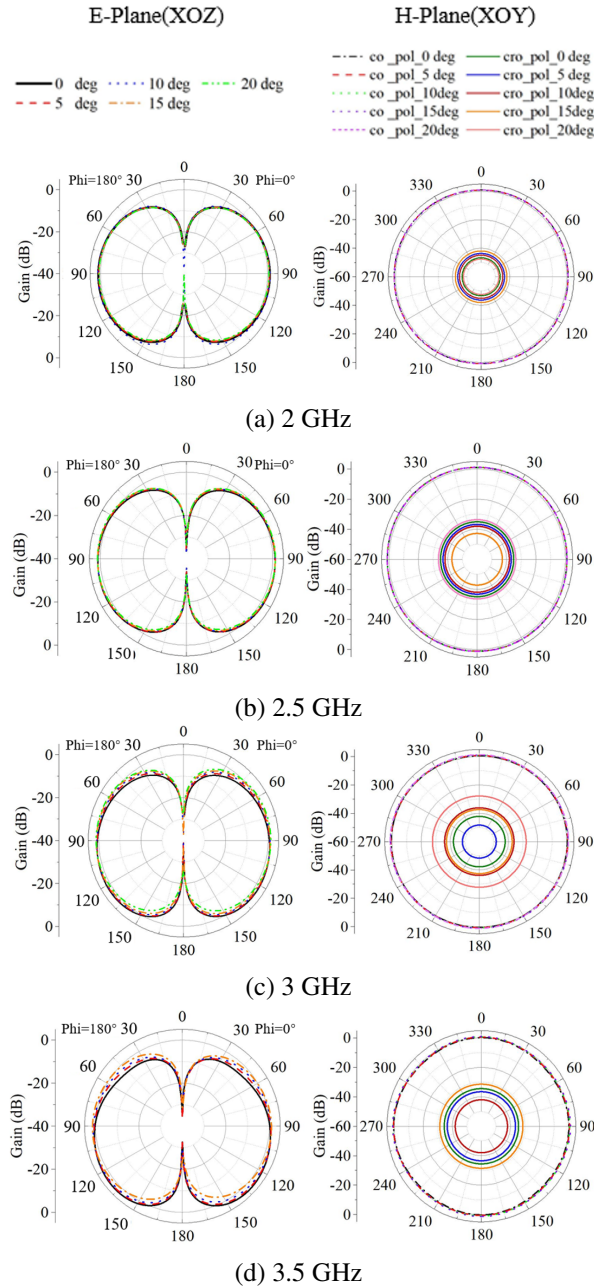


Fig. 11. The effect of parasitic patch on radiation patterns of the antenna.

different taper angles. The cross-polarization level in the horizontal plane is less than -41 dB, respectively. Moreover, in the operating bandwidth, the simulated gain variations for the four taper angles are no more than 1.5 dBi, respectively.

III. EXPERIMENTAL RESULTS

The simulated and measured results of the proposed antenna will be introduced in this section. To verify the

feasibility of the proposed conformal omnidirectional antenna, a prototype with $\alpha = 10^\circ$ is manufactured. The photographs of the fabricated antenna and measured environment are displayed in Fig. 12.

The simulated and measured reflection coefficient is shown in Fig. 13. The measured relative bandwidth of the antenna is 44.36% (2.28 GHz- 3.58 GHz), which is slightly narrower than the simulated one (51.2%) due to the errors caused by fabrication and assembly tolerances. Additionally, the simulated and measured gain is shown in Fig. 14. The result shows that the simulation and test results of the gain are highly consistent. To fix the SMA to the bottom of the antenna, a fixing glue is applied to the welding point on the antenna bottom.

The simulated and measured radiation patterns of the prototype at 2 , 2.5 , 3 , and 3.5 GHz are shown in Fig. 15. It is observed that the antenna can achieve omnidirectional radiation characteristics with the maximum gain variation of 2.2 dBi in the operating frequency range. The main polarization radiation peak gain of the antenna achieves 1 dBi and the cross-polarized gain in the bandwidth is lower than -28 dB.

Table 2 is a chart comparing the proposed work with previous works. Antennae proposed in [3, 5, 6] can achieve omnidirectional radiation characteristics, but antennae with conformal structure and omnidirectional radiation characteristics have difficulty achieving wide operating bandwidth. To expand bandwidth, an antenna conformal to a hemispherical structure is proposed in [11]. However, this antenna cannot achieve omnidirectional radiation and, moreover, the structure of the antenna is complex with significant processing

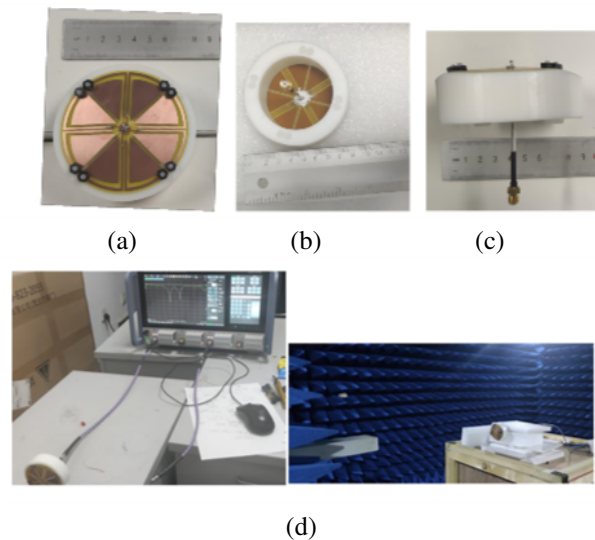


Fig. 12. The photos of the proposed antenna: (a) top view; (b) bottom view; (c) side view; (d) measured environment.

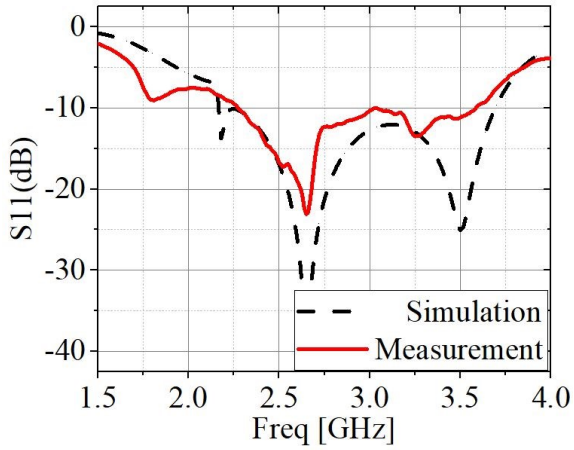


Fig. 13. Simulated and measured results of S11.

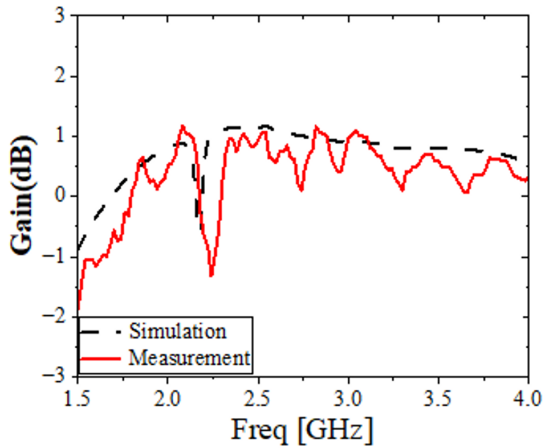
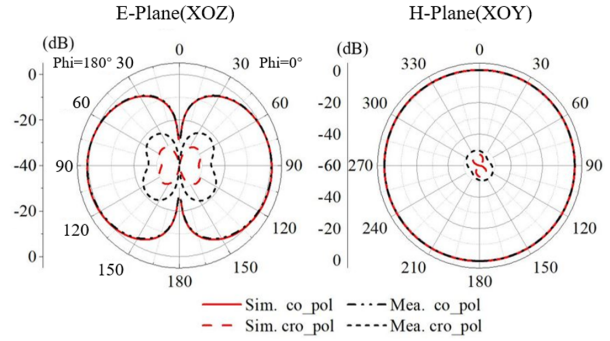


Fig. 14. Simulated and measured gain of the proposed antenna.

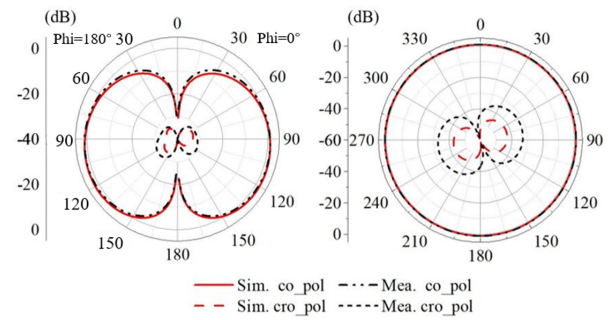
Table 2: Comparison between the proposed and previously reported antennae

Ref.	Size(λ^3)	Radiation Structure	Radiation Direction	BW	Gain (dBi)
[3]	$0.143 \times 0.092 \times 0.016$	conformal	omnidirectional	6.3%	0.5
[5]	$0.8 \times 0.53 \times 0.042$	planar	omnidirectional	1.5%	1.4
[6]	-	conformal	omnidirectional	28%	-2.6
[10]	$0.58 \times 0.58 \times 0.00092$	conformal	omnidirectional	-	2.1
[11]	$0.52 \times 0.52 \times 0.15$	conformal	unidirectional	55.8%	5.8
Prop	$0.53 \times 0.53 \times 0.1$	conformal	omnidirectional	44.4%	1

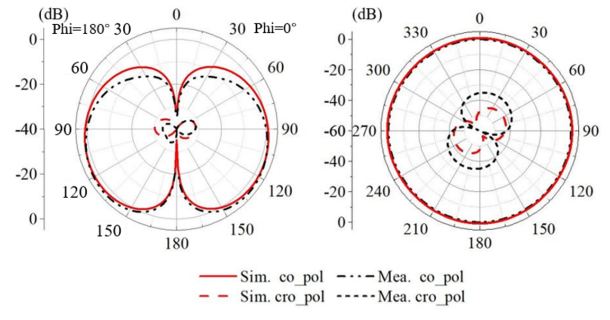
*BW(%):Bandwidth



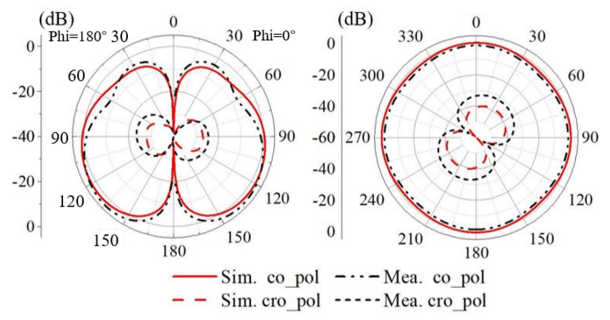
(a) 2 GHz



(b) 2.5 GHz



(c) 3 GHz



(d) 3.5 GHz

Fig. 15. Simulated and measured results of radiation patterns.

and fabrication requirements. Based on a conformal structure, a wideband quadrangular pyramid conformal printed dipole antenna has been designed with the aim of achieving good omnidirectional radiation characteristics in the working frequency band.

IV. CONCLUSION

In this paper, an omnidirectional antenna with a wideband was designed and fabricated. Omnidirectional radiation was realized by exciting four microstrip dipoles with different radiation directions. The dipole units effectively improved the resonance effect of the antenna by introducing parasitic patches. Based on the planar omnidirectional antenna, the radiation characteristics of the omnidirectional antenna at different pyramid angles from 0° to 20° were explored. The measurement results of the prototype with a pyramid angle of 10° were consistent with the simulation ones. High efficiency and small gain variation were obtained in the S-band of 44.36% from 2.28-3.58 GHz. The proposed antenna is therefore considered to be a good candidate for high-efficiency omnidirectional communications applications.

ACKNOWLEDGMENT

We would like to thank the following for their support: the open research fund of National Mobile Communications Research Laboratory, Southeast University (No. 2023D05, Enterprise entrusted project (W2021JSKF0153, W2020JSFW0112), HeFei University of Technology teacher program (JZ2019HGTA0093), An-hui Natural Science Foundation (2208085MF161), and the Fundamental Research Funds for the Central Universities (JZ2021HGTA0144).

REFERENCES

- [1] K. A. Yinusa, "A dual-band conformal antenna for GNSS applications in small cylindrical structures," *IEEE Antennas Wirel. Propag. Lett.*, vol. 17, no. 6, pp. 1056-1059, Apr. 2018.
- [2] H. Y. Liang, H. C. Yang, and J. Zhang, "A cylindrical conformal directional monopole antenna for borehole radar application," *IEEE Antennas Wirel. Propag. Lett.*, vol. 11, pp. 1525-1528, Dec. 2012.
- [3] J. H. Bang, W. J. Kim, and B. C. Ahn, "Two-element conformal antenna for multi-GNSS reception," *IEEE Antennas Wirel. Propag. Lett.*, vol. 16, pp. 796-799, Aug. 2017.
- [4] D. Psychoudakis and J. L. Volakis, "Conformal asymmetric meandered flare (AMF) antenna for body-worn applications," *IEEE Antennas Wirel. Propag. Lett.*, vol. 8, pp. 931-934, July 2009.
- [5] H. Nawaz, X. Liang, M. S. Sadiq, and M. A. B. Abbasi, "Ruggedized surface-mount omnidirectional antenna for supersonic aerial platforms," *IEEE Antennas Wirel. Propag. Lett.*, vol. 19, no. 8, pp. 1439-1442, June 2020.
- [6] G. Byun, C. Seo, B. J. Jang, and H. Choo, "Design of aircraft on-glass antennas using a coupled feed structure," *IEEE Trans. Antennas Propag.*, vol. 60, no. 4, pp. 2088-2093, Jan. 2012.
- [7] B. Feng, K. L. Chung, J. Lai, and Q. Zeng, "A conformal magneto-electric dipole antenna with wide H-plane and band-notch radiation characteristics for sub-6-GHz 5G base-station," *IEEE Access*, vol. 7, pp. 17469-17479, Feb. 2019.
- [8] W. Lei and Y.-X. Guo, "Design of a dual-polarized wideband conformal loop antenna for capsule endoscopy systems," *IEEE Trans. Antennas Propag.*, vol. 66, no. 11, pp. 5706-5715, Nov. 2018.
- [9] H. Yang, X. Liu, and Y. Fan, "Design of broadband circularly polarized all-textile antenna and its conformal array for wearable devices," *IEEE Trans. Antennas Propag.*, vol. 70, no. 1, pp. 209-220, Jan. 2022.
- [10] S. Ahmed, F. A. Tahir, A. Shamim, and H. M. Cheema, "A compact Kapton-based inkjet-printed multiband antenna for flexible wireless devices," *IEEE Antennas Wirel. Propag. Lett.*, vol. 14, pp. 1802-1805, Apr. 2015.
- [11] Y.-D. Yan, Y.-C. Jiao, C. Zhang, Y.-X. Zhang, and G.-T. Chen, "Hemispheric conformal wide beamwidth circularly polarized antenna based on two pairs of curved orthogonal dipoles in space," *IEEE Trans. Antennas Propag.*, vol. 69, no. 11, pp. 7900-7905, Nov. 2021.
- [12] F. F. Ismail, M. A. El-Aasser, and N. H. Gad, "A parasitic hat for microstrip antenna design based on defected structures for multiband applications," *The Applied Computational Electromagnetics Society (ACES) Journal*, vol. 37, no. 5, pp. 568-575, May 2022.
- [13] N. H. Gad and M. Vidmar, "Design of a microstrip-fed printed-slot antenna using defected ground structures for multiband applications," *The Applied Computational Electromagnetics Society (ACES) Journal*, vol. 33, no. 8, pp. 854-860, July 2021.



Zhaoneng Jiang was born in Xuancheng, China. He received the Ph.D. degree from Nanjing University of Science and Technology, Nanjing, China, in 2012. He has been working on numerical methods of computational electromagnetism since 2013. He is currently a Professor at the Hefei University of Technology, Hefei, China. He has authored or coauthored more than 90 papers in refereed international conferences and journals, and has served as Program Committee Member in several international conferences. His current focus is on antenna and microwave devices. (E-mail: jiangzhaoneng@hfut.edu.cn)



Yongxin Sha was born in Anhui, China, in 1996. He is currently working towards the M.E. degree in Electronic Science and Applied Physics at Hefei University of Technology, Hefei, China. He is currently focusing on antenna and microwave device design. (E-mail:

921937992@qq.com)



Liying Nie (corresponding author) was born in Shandong, China, in 1990. She received the Ph.D. degree from the University of Electronic Science and Technology of China. Her research focus is on the theory and design of microwave and millimeter wave antennae. (E-mail: liy-

ingnie@sina.com)



Xiaofeng Xuan was born in Anhui, China, in 1975. He received the M.S. degree from Nanjing University, China. His current focus is on numerical methods of computational electromagnetism. (E-mail:941067868@qq.com)